

Chapter 5

Applications

5.1 INTRODUCTION

There are numerous anthropogenic sources of PAHs, therefore the LIF screening method and the denuder technology developed in this study have many potential applications. A number of these are explored in this chapter, namely the monitoring of emissions from domestic cooking fires, biomass burning, vehicular diesel combustion and industrial processes.

5.2 DOMESTIC FUEL BURNING

5.2.1 Background

In developing countries, fuel is often combusted within homes in order to provide space heating, light, and heat for cooking purposes. It has been estimated that approximately half of the world's population uses solid fuels for cooking and heating (Gustafson et al., 2008). These fuels include wood, paper, charcoal, agricultural wastes (such as maize husks) and animal dung. Combustion conditions are often not optimal, leading to emissions of pollutants including smoke and PAHs. The World Health Organisation has therefore identified indoor air pollution from solid fuel as one of the world's ten major causes of mortality and morbidity (Gustafson et al., 2008). Soot derived from the combustion of biomass fuels (including wood, crop residues, grass, bushes and rice straw) in residential stoves in China was found to have steroid modulating effects, and results showed that PAHs and their derivatives were a major contributor to endocrine disruption (Wu et al., 2002).

The twenty-four hour indoor air levels of a number of PAHs in homes utilizing wood for space heating were significantly higher (3 to 5 times) than in homes without wood-burning appliances (Gustafson et al., 2008). The outdoor air levels of PAHs adjacent to homes combusting this fuel were generally higher than the indoor air levels, and phenanthrene was the PAH at the highest concentration in both indoor and outdoor air (14 ng.m^{-3} and 8.1 ng.m^{-3} , respectively). Fluoranthene and pyrene were also detected in both the indoor and outdoor air samples at concentrations of $\sim 2 \text{ ng.m}^{-3}$, and the gaseous phase accounted for over 90 % of the 3-ring PAHs. Fluoranthene, which has been suggested as a supplementary indicator of carcinogenicity to benzo(*a*)pyrene (Boström et al., 2002), contributed the most of the 3- and 4-ring PAHs to cancer potency, and the sum of the phenanthrene, anthracene, fluoranthene and pyrene concentrations accounted for ~ 80 % of the total PAH concentration.

A maximum total PAH concentration of $2.6 \text{ } \mu\text{g.m}^{-3}$ was obtained in Kenyan kitchen air samples collected onto glass microfibre filters and XAD-2 resin, where charcoal burning stoves were used (Gachanja and Worsfold, 1993). PAH exposures of women cooking on biomass burning stoves were determined in India by means of personal air samplers containing glass fibre filters (Smith et al., 1983). Here only benzo(*a*)pyrene was determined, as this sampling method is not suitable for the more volatile species. PAH monitoring in traditional houses in Burundi revealed that naphthalene was by far the main PAH contaminant, with a mean concentration of $\sim 29 \text{ } \mu\text{g.m}^{-3}$ (Viau et al., 2000). It was also found that the total PAH concentration correlated with the CO concentration and that the mean concentrations of naphthalene, fluorene, phenanthrene and acenaphthalene exceeded $1 \text{ } \mu\text{g.m}^{-3}$.

Domestic fuel burning is also a potential source of PAHs in South Africa, therefore the denuder technology developed in this study was tested in this application in order to assess PAH levels and gas/particle partitioning, which is important for human health impact studies.

5.2.2 Experimental method

a) Sampling

Air samples were collected adjacent to an informal trader in Atteridgeville, Pretoria, whilst chicken was cooked over a coal and wood-fired brazier outdoors, adjacent to a busy roadway in the early evening (19h00).

A quartz fibre filter was punched to the correct size (6 mm o.d.), washed with methanol followed by dichloromethane, and then oven dried at 100 °C for 30 min. The filter was used in conjunction with multi-channel silicone rubber traps in the trap-filter-trap denuder configuration with Teflon connections (see Figure 5.5, section 5.4.3). Sampling was conducted using a portable Gilair sampling pump operating at 517 mL.min⁻¹ for 5 min, at ~1 m above ground level (hand height) and ~5 m from the brazier. After sampling, the filter was transferred to a sealed 2 mL amber vial and the traps were end-capped and wrapped in aluminium foil. Samples were then refrigerated prior to analysis.

b) Analysis

The traps and filter were analysed by thermal desorption-gas chromatography-mass spectrometry (TD-GC-MS) (Gerstel TDS 3 with CIS and Agilent GC 7890A with Hewlett Packard 5975 inert XL MSD). Desorption was from 0 °C (0.2 min) to 270 °C (1.5 min) at 120 °C.min⁻¹ in the solvent vent mode (100 mL.min⁻¹ until 0.2 min). Cryo-focusing of the PAHs was achieved using liquid nitrogen at -40 °C followed by rapid heating at 12 °C.s⁻¹ to 300 °C (10 min). The GC (CIS) inlet was in the split mode (10:1) with helium (Ultra High Purity, Afrox) as the inlet gas. An Agilent HP5 (30 m x 250 µm x 0.25 µm) GC column was used with 68.8 kPa column head pressure. The flow rate through the column was 1.3 mL.min⁻¹ at 40 °C. The GC oven was temperature programmed from 40 °C (10.5 min) at 20 °C.min⁻¹ to 150 °C (0 min) and at 30 °C.min⁻¹ to 300 °C (1 min). The GC-MS transfer line was at 300 °C, the mass scan range was 80-250 atomic mass units (amu), the solvent delay 6.8 min, and the electron multiplier voltage was ~1070 V.

Calibrations were performed by the analysis of 1 $\mu\ell$ injections of mixed PAH standard in toluene (1, 2, 10, 20 and 300 ng for naphthalene and 1, 2, 10, 20 and 40 ng for phenanthrene, anthracene, fluorene and pyrene) onto blank traps or clean filters. NIST library searches were also conducted on the GC-MS data.

5.2.3 Results and discussion

The primary trap obtained from the open fire experiment contained ~16 ng of naphthalene ($6.5 \mu\text{g}\cdot\text{m}^{-3}$), whilst negligible amounts ($< 1.5 \text{ ng}$) were present on the filter and secondary trap, which indicates that no appreciable breakthrough of this analyte occurred with the 2.6 ℓ sampling volume. No particle associated naphthalene was detected in the freshly formed smoke sampled.

For this low sample volume, no significant amounts of the other target PAHs were detected in the samples including the filter, although ~1.5 ng ($0.6 \mu\text{g}\cdot\text{m}^{-3}$) of phenanthrene was detected on the primary trap and ~2 ng ($0.8 \mu\text{g}\cdot\text{m}^{-3}$) of pyrene was found on both the primary and secondary trap. The portion of pyrene present in the secondary trap would have arisen from blow off of particle-associated pyrene from the filter. Our results thus show that in the fresh, particle laden smoke plume, phenanthrene (3 aromatic rings) was present only in the gas phase, whilst the pyrene (4 aromatic rings) was distributed approximately equally between the gas and particle phases. Pyrene, fluorene, anthracene and phenanthrene are regarded as PAH markers for coal and wood combustion (Harrison et al., 1996).

The NIST library searches indicated the presence of both saturated and unsaturated hydrocarbons and their aldehyde and carboxylic derivatives on the primary trap ($Q > 80$), and a smaller number of these compounds were indicated on the secondary trap and filter, as shown in Table 5.1.

Table 5.1: Non-PAH products of domestic fuel burning found in the trap and filter samples, as determined by NIST library comparisons of the TD-GC-MS data.

Compound	R _t (min)	Primary trap	Secondary trap	Filter
Dodecane	15.864	√ (Q91)		
Decanal	15.930	√ (Q96)	√ (Q95)	
1-Pentadecene	16.584	√ (Q87)		
2,4-Decadienal	16.785	√ (Q90)		
Phthalic anhydride	16.826	√ (Q90)		
2-Dodecenal	17.092			√ (Q80)
3-Tetradecene	17.222	√ (Q90)		
Tetradecane	17.265	√ (Q87)		
Dodecanal	17.340			√ (Q90)
Pentadecane	17.797	√ (Q94)		
Tetradecanal	17.867		√ (Q86)	
Cis-7-tetradecen-1-yl acetate	18.161	√ (Q87)		
Tetradecanoic acid	18.963			√ (Q95)
<i>n</i> -Decanoic acid	20.369			√ (Q89)
14-Pentadecenoic acid	20.243	√ (Q91)		

NOTE: Numbers in brackets reflect the quality of the match between the mass spectrum of the sample to that of the library.

This experiment could not be used to assess the efficiency of the denuder system in terms of gas/particle separation, as no target PAHs were present on the filter and the TD-GC-MS analytical method did not lend itself to the detection of even higher boiling PAHs, but it was useful in testing the naphthalene breakthrough volume under practical conditions. The denuder system performed well in that gas phase naphthalene was successfully retained in the primary trap, thus no breakthrough occurred for this PAH, which is not particle associated at room temperature. Should any other PAHs be found in the secondary trap in other experiments performed under similar conditions, it can be inferred that they originated from blow off of PAHs from the particle phase collected on the filter, due to the fact that naphthalene is the PAH with by far the lowest breakthrough volume.

The results also demonstrated the importance of naphthalene as an indicator for PAHs, as it was present at the highest levels, which is in agreement with the literature (Viau et al., 2000). Although the burning was being conducted outdoors in our experiment, indoor fuel burning is also common in South Africa and is even more of concern in terms of potential human health effects.

5.3 DIESEL EXHAUST EMISSIONS

5.3.1 Background

The importance of emissions from road traffic as a source of PAHs has been noted in numerous studies (Wild and Jones, 1995), since the isolation and identification of various carcinogenic compounds in gasoline engine exhaust gas (Hoffmann and Wynder, 1963; Blumer et al., 1977). Road traffic emission studies based in the developing world have been reviewed by Han and Naeher (2006) and the only country on the African continent which has a study included in this review is Egypt, where an average total particulate bound PAH concentration of 32 ng.m^{-3} was reported. Very low levels were found in Croatia (annual average of 1.87 ng.m^{-3}), and very high values were found in Mexico City (median ranged from $60\text{-}910 \text{ ng.m}^{-3}$) in comparison.

In the UK, annual atmospheric emissions of 60 tons of PAHs arise from leaded and unleaded petrol car emissions, with higher emissions from unleaded fuel, due to its higher aromatic fraction (Wild and Jones, 1995). Peak atmospheric PAH concentrations of 1600 ng.m^{-3} have been measured in winter in Los Angeles, during morning rush-hour traffic conditions (Lu et al., 2005).

The composition of diesel emissions is dependent on many factors, including the type of engine, operating conditions, lubricating oil, fuel additives and composition, and emission control systems. Some of the PAHs emitted from diesel engines originate from the fuel itself, as these molecules are relatively refractory and thus a portion survives combustion. Studies by Rhead and Hardy (2003), which utilized a radiotracer technique with the addition of ^{14}C labeled PAHs to the fuel, indicated $< 1.25 \%$ of PAHs arising from the fuel are not combusted

and are emitted. Mean concentrations of the PAHs of interest in diesel fuel are given in Table 5.2, where very high concentrations of naphthalene are evident. Another study also found naphthalene to be the predominant PAH present in both diesel (up to 1600 ppm) and gasoline (up to 2600 ppm) (Marr et al, 1999).

Table 5.2: Mean PAH concentrations in class A2 diesel fuel (Rhead and Hardy, 2003).

PAH	Mean concentration (ppm)
Naphthalene	1292
Fluorene	571
Phenanthrene	945
Anthracene	19
Fluoranthene	36
Pyrene	83
Chrysene	41
Benzo(<i>a</i>)pyrene	0.4

Pyrosynthesis of PAHs during the high temperature combustion conditions also contributes to emission levels, although most of the combustion products are oxidized prior to emission (USA EPA, 2002). Pyrosynthesis has been found to be most prominent under high speed and load conditions (Rhead and Hardy, 2003). The concentrations of selected PAHs associated with diesel particles from light duty diesel engine exhausts, are summarized in Table 5.3.

Table 5.3: PAHs extracted from diesel particles from light duty diesel engine exhausts (USA EPA, 2002).

PAH	Concentration (ng.mg ⁻¹ extract)
PhA	2186 – 4883
FlA	3399 – 7321
Py	3532 - 8002

Other factors which have been found to influence PAH emissions from automobiles include the engine power (with increased emissions at higher engine powers) and the aromatic

content of the fuel, particularly the C₉ and C₁₀ aromatics. Higher PAH emissions were found from low sulphur fuel combustion, and very rich and very lean air:fuel ratios lead to high emissions of particulates and PAHs. A close relationship between PAH emissions and the age of the car has also been recorded, where the PAH emissions increased with increase in car speed of high mileage cars (Nikolaou et al., 1984). In another study, PAH emissions were found to increase with increased mileage but no correlation was found between PAH exhaust emissions and the amount of PAHs in the lubricating oil (Stenberg, 1985).

When a cold engine is started, the emission rates of PAHs are similar for both diesel and petrol engines, and are ~six times higher than with warm starts. With warm engine starts, however, the emissions from diesel engines were higher than that of petrol engines, although this conclusion is complicated by the difference in volume of exhaust gas emitted from each of these engine types, as the higher volume of diesel emissions has a diluting effect on the PAH concentrations (Nikolaou et al., 1984). The elevated emissions under cold start conditions were found not to be related to the combustion chamber wall temperature, but were rather the result of the low air:fuel ratio and higher engine load which both result in increased emissions of PAHs (Pedersen et al., 1980). It should be noted that a cold start is generally defined as the starting of a vehicle which has been standing for at least 12 hours at room temperature (Stenberg, 1985).

In terms of particle size, approximately 50 – 90 % of the number of particles in diesel exhaust are in the ultrafine size range (0.005 – 0.05 µm, with the mode at 0.02 µm), although in terms of mass, ultrafine diesel particulate matter accounts for only 1 – 20 % of the total mass. Approximately 80 – 95 % of the diesel particulate mass is in the range 0.05 – 1.0 µm, with the mean particle diameter of ~0.2 µm (USA EPA, 2002). The distribution of PAHs is shifted to smaller particle sizes for lower vehicle loads (Zielinska et al., 2004). Particle losses in the silicone rubber trap denuder developed in this study would be minimal for these particle size ranges (< 5 % loss for particles > 0.006 µm and 0 % for particles > 0.05 µm), as discussed in Chapter 4.

Krieger and Hites (1992) utilized a denuder based on capillary columns to sample diesel exhaust 0.2 m from the exhaust pipe of an idling diesel bus (at approximately 35 °C), yielding a 40 ℓ sample volume. Lower vapour pressure PAHs were not present in the denuder

itself, indicating that impaction of particles was not significant and that transmission of particles was effective. It was noted that the sample was fresh, thus there was not sufficient time for equilibrium partitioning between the vapour and particle associated phases. Phenanthrene, for example, was found in equal concentrations in the two phases. *n*-alkanes in the diesel exhaust were used to assess breakthrough, particularly of analytes which had a retention index of < 1300, which were distributed between the denuder and the post-filter PUF plug. Compounds with retention indices of between 1300 and 1600 were only present on the denuder, and thus were present in the vapour phase only. Analytes with retention indexes higher than this were associated with particles, and were completely associated with particles at retention indices > 2200 (Krieger and Hites, 1992).

Sampling the entire effluent is an alternative to the use of a dilution tunnel, and eliminates the complexities associated with isokinetic sampling (Boubel and Ripperton, 1963). However, the USA EPA requires dilution sampling for testing of diesel engines (Lipsky and Robinson, 2005) therefore various large and complex dilution sampling systems have been developed by car manufacturers, which operate at $\sim 1000 \text{ l}\cdot\text{min}^{-1}$ with mixing tunnels > 1 m long. More portable systems have also been designed, which have dilution tunnels < 1 m long and operate at flow rates of $\sim 175 \text{ l}\cdot\text{min}^{-1}$ (Lipsky and Robinson, 2005). Dilution samplers should simulate atmospheric dilution, minimize contamination and sampling losses, as well as provide adequate residence time for aerosol processes to occur. Measurements of CO_2 in the undiluted and diluted exhausts may be employed to determine the dilution ratio (Lipsky and Robinson, 2005). Dilution may, however, effect the particle size distribution and partitioning of semi-volatile organic compounds arising from diesel combustion (Lipsky and Robinson, 2006). To overcome these problems, Benner et al. (1989) sampled in a roadway tunnel, where concentrations of 18; 20; and $27 \text{ ng}\cdot\text{m}^{-3}$ were found for phenanthrene; fluoranthene and pyrene, respectively.

The distribution of PAHs between the gas and particle phases determined from samples taken in a dilution tunnel at $\sim 30 \text{ }^\circ\text{C}$ for both gasoline and diesel exhausts is shown in Table 5.4. It is evident that a higher fraction of PAHs are associated with particles in the case of diesel exhausts (which tend to emit more particles), as compared to gasoline (Stenberg, 1985).

Table 5.4: Percentage distribution of PAHs between the gas and particle phases in gasoline and diesel exhausts (Stenberg, 1985).

PAH	Gasoline		Diesel	
	% gas phase	% particles	% gas phase	% particles
PhA	95	5	53	47
FlA	36	64	9	91
Py	25	75	6	94

Zielinska et al. (2004) found that 80-90 % of the four-ring PAHs (including fluoranthene and pyrene) were present in the 8-channel, polystyrene-divinylbenzene (XAD-4) coated denuder portion of a sampling train used to monitor vehicular emissions, and were therefore in the gas phase under engine idling conditions. Under high loads, a much larger portion of these compounds were partitioned to the particle phase. It should be noted that an extensive XAD-4 cleaning procedure was needed prior to use, and organic solvent sample extraction was required prior to analysis. A sampling flow rate of 90 l.min^{-1} was used and the exhaust gases were diluted prior to sampling. Naphthalene breakthrough under these conditions was found to be ~20 %, which was considered acceptable as the flow rate was optimized for phenanthrene to minimize particle loss to the walls of the denuder, as well as evaporative losses of more volatile PAHs from particles during their residence time in the denuder.

Continuous, real-time instruments, based on a photoelectric aerosol sensor have been used to determine total particulate PAH concentrations in diesel emissions, impacted ambient, and occupational exposure sites, including a bus terminal and a distribution centre (Marr et al., 2004). Median total particulate concentrations along Mexico City's roadways ranged from 60 to 910 ng.m^{-3} , with a detection limit of 1 ng.m^{-3} . It was noted that the instrument is slightly more sensitive to larger PAHs, due to their lower photoionisation energies.

Kozielet al. (2001) compared needle trap devices to PDMS SPME fibres in sampling diesel vehicle exhaust emissions and found that the reproducibility for SPME was slightly better, averaging at 25 % for targeted PAHs. Uncertainties were ascribed to sampling errors

including short sampling times (2 min), small sampling volumes (20 mL), and turbulence in the sampling train used.

It is clear from this discussion that there are many factors which contribute to the emissions of PAHs from diesel vehicles, which makes comparison of results from different studies difficult. Due to the potential contribution of vehicular emissions to atmospheric PAH levels in South Africa, the use of our PDMS-based denuder technology was investigated in this application.

5.3.2 Experimental method

Quartz fibre filters were punched to the correct size (6 mm o.d.), washed with methanol followed by dichloromethane, and then oven dried at 100 °C for 30 min. These were used in conjunction with multi-channel silicone rubber traps in the following three sampling configurations and sampling flow rates:

- i) Trap-filter-trap (433 mL.min⁻¹)
- ii) Tube-filter-trap (443 mL.min⁻¹)
- iii) Trap-trap (366 mL.min⁻¹).

Teflon tubing connections were used in each case. Sampling of the exhaust of an idling diesel vehicle (2006 Citroen C3, 1.4) was performed under cold start conditions for 11 min, by means of battery-operated portable Gilair sampling pumps, as shown in Figure 5.1. The weather conditions during sampling were clear and sunny, with a moderate gusty wind. The ambient temperature was 28 °C. After sampling, the filters were transferred to sealed 2 mL amber vials and the traps were end-capped and wrapped in aluminium foil. Samples were then refrigerated prior to analysis by TD-GC-MS according to the details given in section 5.2.2 (b).



Figure 5.1: Sampling of diesel vehicle emissions with multi-channel silicone rubber traps and quartz fibre filters. Sampling configurations from left to right were: tube-filter-trap; trap-filter-trap and trap-trap.

5.3.3 Results and discussion

The results of the diesel vehicle emission monitoring experiments are summarized in Table 5.5. The primary trap of the trap-filter-trap sampling configuration contained significantly more naphthalene than any of the other traps. This was due to the positioning of this sampling system, which placed the trap closer to the emission source than the other two sampling configurations (refer to Figure 5.1). This impacted on the results due to the gusty wind conditions experienced during sampling. The same amount of naphthalene was collected in the primary trap of the trap-trap configuration and in the trap of the tube-filter-trap configuration, which confirmed that no gas phase naphthalene was adsorbed onto the filters during sampling. Although the filter was blackened due to particle loading, no particle-associated naphthalene was found at the sampling temperature (28 °C), as was expected due to its volatility. Visual inspection of the filters and traps showed that particles had been successfully collected on the filters and had not been lost in the primary trap. No breakthrough of naphthalene was evident in the secondary traps at the low sample volumes employed (4.0 to 4.9 ℓ), and no fluorene, anthracene, phenanthrene or pyrene were detected in any of the samples. As a result of the low sample volumes and the TD-GC-MS analytical method

employed, which did not allow for the detection of heavier boiling PAHs as mentioned under section 5.2.3, the sampling system could not be effectively tested as a denuder for the heavier PAHs in this experiment.

Table 5.5: Naphthalene concentrations ($\mu\text{g}\cdot\text{m}^{-3}$) in diesel vehicle emissions sampled onto multi-channel silicone rubber traps and quartz fibre filters with TD-GC-MS analysis.

SAMPLING CONFIGURATION	PRIMARY TRAP	FILTER	SECONDARY TRAP
i) Trap-filter-trap	4.3	nd	nd
ii) Tube-filter-trap	na	nd	1.8
iii) Trap-trap	1.8	na	nd

na = not applicable; nd = not detected (<1 ng).

The NIST library search indicated that hydrocarbons and their oxidized derivatives may have been present in the samples, including aldehydes, carboxylic acids and esters ($Q > 80$) as shown in Table 5.6.

Table 5.6: Non-PAH products of diesel vehicle emission trap and filter samples, as determined by NIST library comparisons of the TD-GC-MS data.

Compound	R _t (min)	Filter (trap/filter /trap)	Secondary trap (trap/filter /trap)	Filter (tube/filter /trap)	Trap (tube/filter /trap)	Primary (trap/ trap)	Secondary (trap/ trap)
Decanal	15.930	√ (Q90)	√ (Q96)				√ (Q94)
n-Decanoic acid	17.065						√ (Q94)
Tetradecane	17.265				√ (Q81)		
6,10-Dimethyl-5,9-undecadien-2-one	17.582	√ (Q81)	√ (Q80)				
Dodecanoic acid	18.089						√ (Q99)
Hexadecane	18.265				√ (Q96)		
Tetradecanoic acid	18.922	√ (Q92)	√ (Q90)	√ (Q94)	√ (Q93)		√ (Q97)
Isopropyl myristate	19.173			√ (Q87)			
14-Pentadecenoic acid	19.301		√ (Q90)				
1-Nonadecanol	19.396						√ (Q91)
Hexahydro-1-oxa-cyclopropa(<i>d</i>)inden-2-one	19.591	√ (Q80)					
Pentadecanoic acid	19.652					√ (Q86)	
Oxybenzone	20.026	√ (Q91)		√ (Q96)	√ (Q90)		√ (Q97)
1-Hexadecanol	20.089						√ (Q91)
Oxacyclotridecan-2-one	20.241		√ (Q90)				
2-Propenoic acid	20.374	√ (Q91)		√ (Q91)		√ (Q83)	√ (Q91)
Thianaphthene-2-carboxylic acid	20.833	√ (Q83)			√ (Q83)		

NOTE: Numbers in brackets reflect the quality of the match between the mass spectrum of the sample to that of the library.

5.4 SUGAR CANE BURNING

5.4.1 Background

Sugar cane (*Saccharum officinarum*) is a tall perennial grass (as shown in Figure 5.2), which is cultivated in approximately 200 countries for sucrose production. In South Africa, approximately 430 000 hectares of sugar cane is currently under cultivation, and this is mainly distributed along the coastal region of KwaZulu-Natal, with a number of inland areas in both KwaZulu-Natal and Mpumalanga (South African Sugar Association, 2006).



Figure 5.2: Sugar cane (*Saccharum officinarum*) growing in KwaZulu-Natal, South Africa.

In general, agricultural open burning is used as a rapid means of disposing of crop residues, releasing nutrients for the next growth cycle and clearing land. In the case of sugar cane, burning removes dry leaves and eradicates any pests (such as snakes and cane rats) which may be present in the plantation prior to manual harvesting, which is the primary harvesting method in use in South Africa. Burning makes manual harvesting of the moisture-

rich stalks using knives or machetes easier, which has financial benefits. It also reduces the unused leaf mass that must be transported to the sugar mills, and may increase the sugar content by weight, due to evaporation of water. The roots (or canes) which remain post harvest send up new stalks called ratoons, which grow and develop into the new harvest.

Although the pre-harvest sugar cane burns have time saving and thus financial benefits, they are also potential sources of large amounts of air pollutants (Figure 5.3), thus monitoring of these events is important especially as sugar cane is cultivated close to residential areas, particularly in KwaZulu-Natal. Numerous PAH congeners have been identified in fly soot extracts derived from sugar cane burns (Zamperlini et al., 1997), with phenanthrene, fluoranthene and pyrene being major contributors (Godoi et al., 2004a), and particulate matter from sugar cane burning has been found to be at least as toxic as that produced by traffic (Mazzoli-Rocha et al., 2008). Analysis of particulate matter arising from the combustion of sugar cane leaves and bagasse in controlled experiments gave concentrations of up to 242 ng.m^{-3} of phenanthrene, 369 ng.m^{-3} of anthracene, 341 ng.m^{-3} of fluoranthene and 182 ng.m^{-3} of pyrene (dos Santos et al., 2002).



Figure 5.3: Particle laden plume arising from a sugar cane burn in KwaZulu-Natal.

Emissions from open burning, on a mass of pollutant per mass of fuel basis, are greater than those from well-controlled combustion sources, although biomass open burning sources typically emit less PAHs than combustion of anthropogenic materials (Lemieux et al., 2004). Open burning raises human health concerns because the emissions are released at ground level and not through tall stacks which may aid dispersion. They are also episodic in time or season and enforcement of bans or regulatory controls is difficult. The fuel source is often heterogeneous which complicates emission estimates (Lemieux et al., 2004). The moisture content of the fuel (i.e. the sugar cane vegetation), the meteorological conditions, and the topographical features of the burn site all contribute to modify the burning conditions as the fire spreads, thus different degrees of combustion efficiency are attained during a burn. The dry vegetation is usually combusted first, releasing energy which dries green, live material, which is subsequently burnt.

Open combustion sources produce particles of a wide size range, which depends in part on the rate of energy release of the fire. In high-intensity fires, a bimodal particle volume distribution has been noted, with peaks around $0.3 \mu\text{m}$ and $> 10 \mu\text{m}$. The larger size fraction may be composed of ash and partially burnt plant material, and is entrained in the smoke plume due to the turbulence arising from the high-intensity fire (USA EPA, 1996). As discussed in Chapter 4, particles of these sizes should be fully transmitted by the multi-channel silicone rubber trap denuder system. The fine, respirable particle fraction has been found to dominate in sugar cane burn samples and may therefore impact on human health (Godoi et al., 2004b). The PAH particle-phase concentrations and PAH particle fraction are strongly influenced by burning conditions (Jenkins et al., 1996).

Total particulate PAH concentrations of up to $342 \text{ ng}\cdot\text{m}^{-3}$ were measured in winter in Brazil during seasonal sugar cane burning events (de Almeida Azevedo et al., 2002), where phenanthrene was the most abundant PAH ($2.15 - 21.5 \text{ ng}\cdot\text{m}^{-3}$). Higher concentrations of the more unstable PAHs, (which contain five-membered rings, such as fluoranthene), than that of the more stable isomers containing only six-membered rings (such as pyrene), may indicate a combustion or anthropogenic source (dos Santos et al., 2002). PAHs have been investigated as potential tracers for biomass combustion products, where phenanthrene, fluoranthene and pyrene were found in aerosols from sugar cane burns (Ballentine et al., 1996).

Due to the rate of occurrence of sugar cane burning events in South Africa and the proximity of residents to the sugar cane growing areas, it was deemed important to consider this potential source of PAH emissions. The PDMS denuder system was tested in this application, and the sample traps were analysed by both the LIF screening method and by TD-GC-MS.

5.4.2 Experimental method

Two multi-channel silicone rubber traps were employed in series, separated by a quartz fibre filter, which was held in place with a Teflon connector, in order to sample emissions from a sugar cane burn at Umhlali on the KwaZulu-Natal North Coast on 14 August 2006. A Gilair portable sampling pump equipped with a low flow module was used to sample air in the emission plume for 10 minutes at $500 \text{ mL}\cdot\text{min}^{-1}$, as shown in Figure 5.4. Sampling was then repeated with a second set of traps and a quartz fibre filter (Figure 5.5a). After sampling, the traps were end-capped, wrapped in aluminium foil and refrigerated prior to analysis.



Figure 5.4: Sampling train with pump, located approximately 20 m from the burn front.

One set of silicone rubber traps and quartz fibre filter was thermally desorbed using a thermal desorber system (TDS) and the desorbed PAHs were cryogenically focused via a

cooled injection system (CIS) (Gerstel) on 4 September 2006. The traps and filter were desorbed from 30 °C (3 min) to 280 °C (10 min) at 60 °C.min⁻¹ in the splitless flow mode. Cryo-focusing of the PAHs was achieved using liquid nitrogen at -20 °C at 12 °C.s⁻¹ to 300 °C (10 min). The GC-MS system was an Agilent GC 6890A coupled to a Hewlett Packard 5973 mass selective detector (MSD). The GC inlet was in the solvent vent mode with helium (Ultra High Purity, Afrox) as the inlet gas. The vent flow was 60 mL.min⁻¹, the vent pressure 65 kPa until 0 min, and the purge flow to split vent was 60 mL.min⁻¹ at 1 min. The GC column was from Restek RTX1-MS (30 m x 250 µm x 25 µm) and the column head pressure was 65 kPa in the constant pressure mode using helium as the carrier gas. The velocity of the gas was 39 cm.s⁻¹ (1.1 mL.min⁻¹) at 60 °C. The GC oven was temperature programmed from 60 °C (5 min) at 20 °C.min⁻¹ to 280 °C (5 min). A post run was performed at 300 °C (2 min) at 100 kPa. The GC-MS transfer line was at 300 °C, the mass scan range was 45-450 atomic mass units (amu) and the electron multiplier voltage 1700 V.

The second set of traps and filter were analysed by LIF on 7 September 2006, using the method described in Chapter 3 and an excitation wavelength of 292 nm. These traps (which had been analysed by LIF), were then re-capped and stored in a refrigerator at 5 °C and the filter was stored at room temperature in a sealed 2 mL amber vial until 26 February 2009 when the samples were analysed by TD-GC-MS, according to the procedure detailed in section 5.2.2 (b). A mixed PAH standard was used for calibration purposes (0.1; 1 and 10 ng).

5.4.3 Results and discussion

It is acknowledged that the sampling system should have been placed vertically to ensure efficient denudation (as discussed in Chapter 4), however, the horizontal positioning used did not appear to have significantly impacted on the results. Visual inspection of the traps after sampling clearly showed that the fine particles had passed through the first silicone trap, and were present on the filter, as shown in Figure 5.5b). The system served as a denuder in that gas phase analytes were trapped by the first silicone rubber trap, whilst particle-bound analytes were trapped by a quartz fibre filter. Any analytes which entered the gas phase after impacting on the filter were trapped by the second silicone rubber trap, as were any gas phase analytes which broke through the first trap.

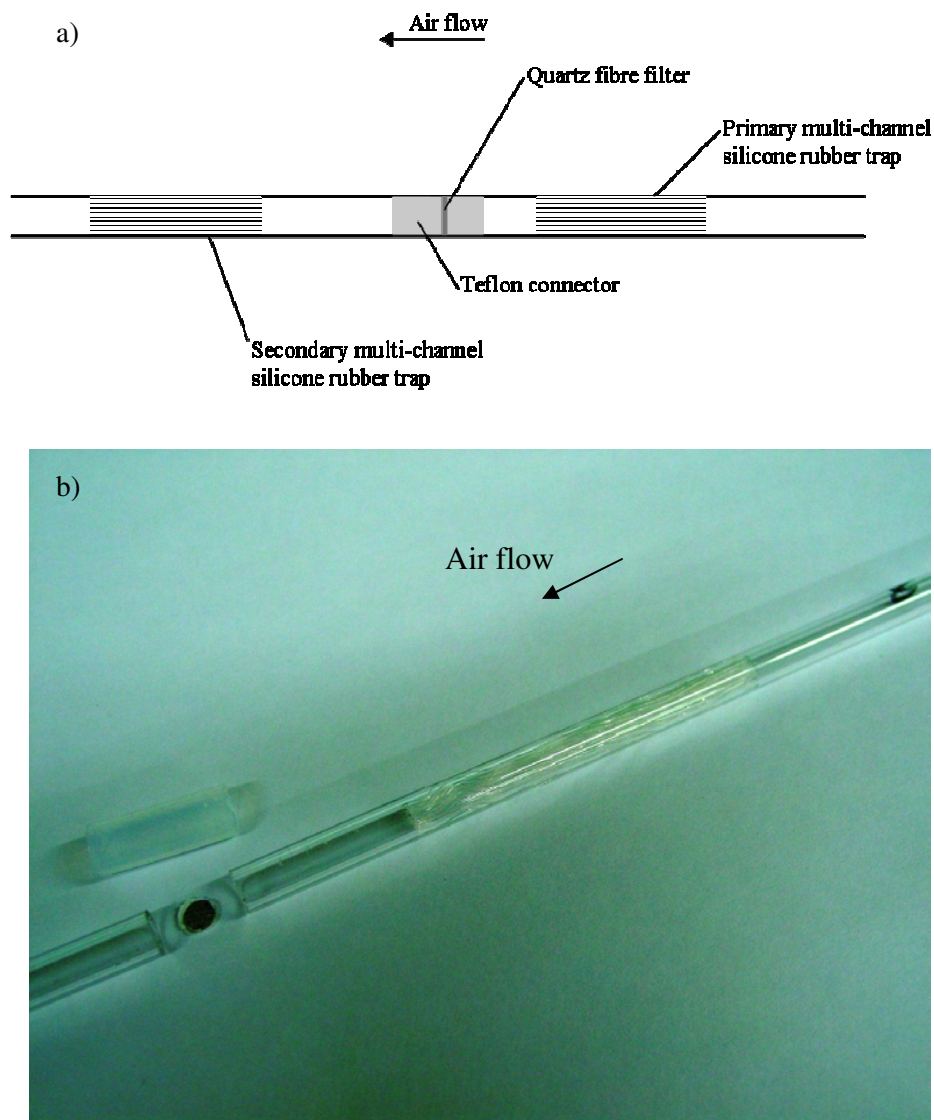


Figure 5.5: a) Multi-channel silicone rubber traps and a quartz fibre filter employed in the denuder configuration. b) Dismantled silicone trap system after sugar cane burn sampling, with no particles evident on the trap, whilst the filter which was downstream of the trap is heavily loaded with particles.

LIF results of the traps focused on naphthalene, which showed a concentration profile through the sampling system (refer to Figure 5.6), with possible overlap of heavier PAH emission spectra at the inlet side of the first trap. The samples therefore screened positive for naphthalene via the LIF method, indicating the need for quantitative GC-MS analysis. This experiment proved the concept of our LIF method as a screening tool. The profile in Figure 5.6 also indicates the possibility of spectral deconvolution by the sequential subtraction

of spectra obtained consecutively down a trap in order to enhance resolution. This is possible as separation of different analytes occurs as the air sample moves through the PDMS trap in the same manner as in chromatographic frontal analysis. Subtraction of fluorescence spectra has been shown to be a useful means of enhancing resolution in the analysis of complex mixtures of aromatic compounds by liquid chromatography with a fluorometric photodiode array detection system (Gluckman et al., 1985), for example.

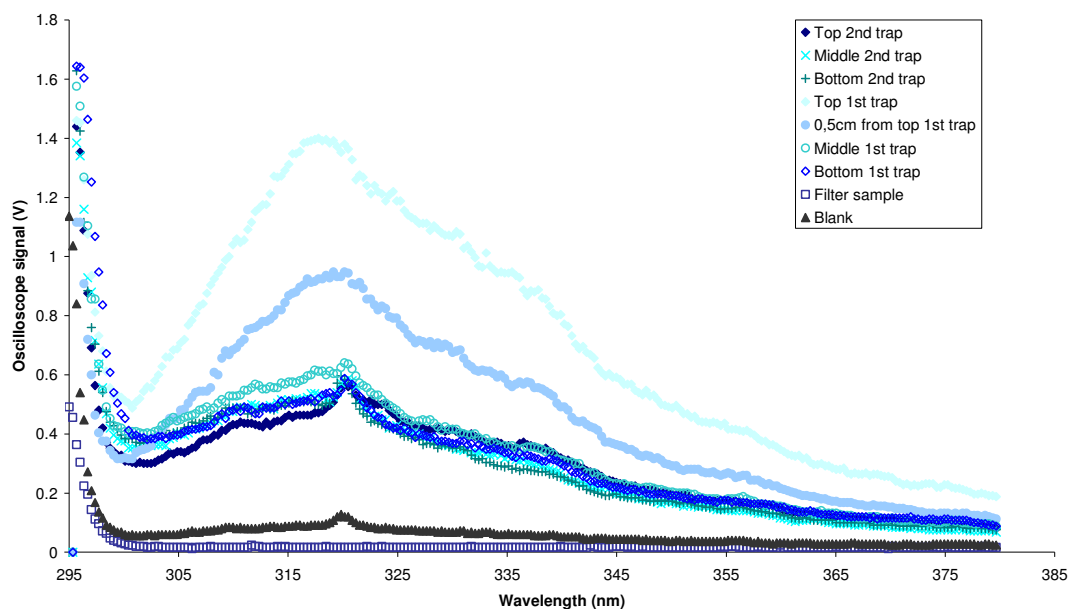


Figure 5.6: Naphthalene fluorescence spectra of the first and second traps at different positions along their lengths (where the top indicates the sample inlet side), and the filter, with excitation at 292 nm.

The TD-GC-MS results obtained on 4 September 2006 are summarized in Table 5.7. There was significant co-elution with respect to the naphthalene peak using this GC method, thus results are semi-quantitative. The first trap contained ~ 1 ng ($0.2 \mu\text{g}\cdot\text{m}^{-3}$) of naphthalene (comparison with peak area of a 0.1 ng standard analysis), whilst very small amounts were present on the filter, as expected for this volatile compound. Better results were obtained for phenanthrene; fluoranthene and pyrene. Due to their lower volatility, higher concentrations of these analytes were present in the particle phase. Other studies have similarly shown that the

naphthalene content of sugar cane soot was a factor of ~ 7 times lower than that of phenanthrene, fluoranthene and pyrene (Godoi et al., 2004a), with concentrations ranging from 0.42 ng.m^{-3} for naphthalene to 3.3 ng.m^{-3} for fluoranthene.

Table 5.7: Sugar cane burn PAH TD-GC-MS results (analysis on 4 September 2006), indicating concentrations (for naphthalene) or relative % contributions (for the other PAHs).

Parameter	Naphthalene	Phenanthrene	Fluoranthene	Pyrene
R_t (min)	9.7	14.2	15.8	16.1
1 st trap (gas phase)	$\sim 1 \text{ ng}$	81 %	71 %	65 %
Filter (particle bound)	$< 0.1 \text{ ng}$	2 %	9 %	12%
Second trap	Co-elution	17 %	20 %	23 %

The percentage of phenanthrene, fluoranthene and pyrene present in the gas and particle phases compare favourably with those reported for ambient air samples in the literature (refer to Table 4.3 in Chapter 4), although a lower portion of the total pyrene was found in the gas phase in this study, possibly due to the high particulate loading in the smoke plume. Most sugar cane PAH monitoring has focused on particulates, therefore data on gas/particle partitioning for this source is rather limited.

The TD-GC-MS results obtained on 26 February 2009 proved the stability of trapped samples, as naphthalene (the most volatile PAH) was still present on the traps after refrigerated storage for over two years. The primary trap was found to contain 13 ng of naphthalene ($2.6 \mu\text{g.m}^{-3}$) and 3.3 ng of phenanthrene ($0.7 \mu\text{g.m}^{-3}$), whilst the secondary trap contained 1.8 ng of naphthalene ($0.4 \mu\text{g.m}^{-3}$), which indicates that some breakthrough had occurred at the 5ℓ sampling volume. Breakthrough was also evident from the LIF results (Figure 5.6)

Better resolution was obtained with this GC-MS method, thus more confidence could be placed on the resulting naphthalene concentrations than in those determined previously, which would seem to have been underestimated. The two sample sets were also taken sequentially, which would also contribute to the inter-sample variation.

The filter samples had been stored in 2 ml amber vials at room temperature, therefore volatilization losses were expected. No target PAHs were found on the filter, and the NIST

library search on the GC-MS data indicated that esters and carboxylic acids of hydrocarbons, as well as aromatic aldehydes and esters may have been adsorbed onto the particulate matter ($Q > 80$). The possible presence of both phenol derivatives and oxidized hydrocarbon and aromatic derivatives were evident from the library search results of the primary trap data. In addition, biphenyl ($Q = 87$), *o*-hydroxybiphenyl ($Q = 97$), and 2-methyl naphthalene ($Q = 90$) may also have been present on the primary trap. The secondary trap may have contained *o*-hydroxybiphenyl ($Q = 96$), and 2,6-diisopropylnaphthalene ($Q = 94$).

The multi-channel silicone rubber trap denuder system and the LIF screening method were therefore successfully tested in this application, where PAH partitioning between the gas and particle phase was evident.

5.5 INDUSTRIAL EMISSIONS

5.5.1 Background

Industrial atmospheric emissions may contain PAHs when processes involve organic compounds and elevated temperatures, such as those of incinerators, diesel-fired boilers and oil refineries. A sampling campaign was therefore performed in the Vaal region of South Africa, which has been declared a priority area in terms of air quality under the National Environmental Management: Air Quality Act (Act No. 39 of 2004) (Department of Environmental Affairs and Tourism, 2006). A relatively low atmospheric particulate load was expected therefore the denuder sampling configuration was not employed. Breakthrough conditions were, however, tested by sampling onto two traps in series.

5.5.2 Experimental method

Prior to sampling, blank multi-channel polydimethylsiloxane rubber sample traps were analysed by LIF and TD-GC-MS. Gas phase air samples were collected actively onto two traps in series, using portable Gilair personal sampling pumps. Sampling was performed in triplicate at roughly the breathing zone height at three locations in the vicinity of an oil refinery:

- Site 1: At the fence-line down wind of the oil refinery
- Site 2: Adjacent to a power station and surrounded by various industries in the area, but upwind of all these sources
- Site 3: Similar location to site 1, but slightly further east.

In order to evaluate breakthrough volumes and optimal sampling flow rates, three different sampling flow rates were employed at each site as well as different sampling intervals (10 or 25 min), such that sample volumes ranged from 3.7 to 31.9 ℓ, as shown in Table 5.8.

Table 5.8: Sampling conditions for the monitoring of PAHs in industrial atmospheric emissions.

Pump	Flow rate (mℓ.min ⁻¹)	Sampling interval (min)	Total sample volume (ℓ)
A	184	25	4.6
B	370	10	3.7
C	1276	25	31.9

The samples (including a field blank) were analysed by LIF using 292 nm excitation radiation according to the method developed in Chapter 3, and the emission spectra were recorded from 295 to 465 nm. A positive or negative screening result was determined by comparing the fluorescence signal at 323 nm of the trap blank with that obtained after sampling. The traps were then analysed directly by TD-GC-MS, using the method described in section 5.2.2 (b), and six target PAHs (naphthalene, phenanthrene, pyrene, fluoranthene, fluorene and anthracene) were quantified using a mixed PAH standard for calibration purposes (0.1; 1; 10 and 100 ng).

5.5.3 Results and discussion

No PAHs were detected on the blank traps prior to sampling by LIF and TD-GC-MS. During sampling, it was noted that the wind speed was moderate and that weather conditions were sunny. A strong chemical (cresol-like) smell was noted at the first (where the smell came in wafts) and third sampling sites, whilst no particular odours were evident at the second site.

The various sampling flow rates and sample volumes allowed for the successful confirmation of laboratory derived breakthrough volumes for the analytes of interest, as it was evident that breakthrough only occurred at the highest sampling flow rate, where the corresponding sample volume was 31.9 ℓ (Table 5.9).

The TD-GC-MS results at the first sampling site indicated a naphthalene concentration of between $\sim 10 \mu\text{g}\cdot\text{m}^{-3}$ (for the 25 minute samples), and $\sim 25 \mu\text{g}\cdot\text{m}^{-3}$ (for the 10 minute sample). This difference is likely due to variations in concentration of PAHs in the air over the sampling interval, as noted from the wafting chemical smell during sampling. No other target PAHs were detected.

The target PAH concentrations were all below the limit of detection of the GC-MS for the samples from the second site ($< 0.1 \text{ ng on trap}$). This was to be expected, as sampling was conducted upwind of the industrial sources.

The industrial odour evident at sampling site 1 was less evident during sampling at site 3 (taken 1 hr & 20 min later). This was reflected in the results, as the naphthalene concentration was $\sim 3 \mu\text{g}\cdot\text{m}^{-3}$. Excellent reproducibility was found between traps in this case, indicating a more constant concentration over the sampling interval. No other target PAHs were detected.

An example of a fluorescence spectrum of a primary trap which screened positive is shown in Figure 5.7.

Table 5.9: Industrial monitoring LIF screening and TD-GC-MS naphthalene results for the three sampling sites and different sampling volumes.

Analytical method	4.6 l sampling volume		3.7 l sampling volume		31.9 l sampling volume	
	25 min at 184 mL.min ⁻¹		10 min at 370 mL.min ⁻¹		25 min at 1276 mL.min ⁻¹	
	Primary trap	Secondary trap	Primary trap	Secondary trap	Primary trap	Secondary trap
<i>Sampling site 1</i>						
LIF	Positive	Positive	Positive	Negative	Positive	Positive
TD-GC-MS	44 ng 9.6 µg.m ⁻³	ND	95 ng 26 µg.m ⁻³	ND	214 ng 6.7 µg.m ⁻³	102 ng 3.2 µg.m ⁻³
<i>Sampling site 2</i>						
LIF	Negative	Negative	Negative	Negative	Negative	Negative
TD-GC-MS	ND	ND	ND	ND	ND	ND
<i>Sampling site 3</i>						
LIF	Positive	Positive	Negative	Positive	Positive	Positive
TD-GC-MS	12 ng 2.6 µg.m ⁻³	ND	11 ng 3.0 µg.m ⁻³	ND	82 ng 2.6 µg.m ⁻³	16 ng 0.5 µg.m ⁻³
ND = not detected						

Three false positives were recorded with the LIF screening. All of these were for secondary traps sampled at contaminated sites, therefore it is possible that non-target molecules of fairly high volatility, which contained fluorophores, were present in these traps. The field blank, however, also gave a false positive, although no naphthalene was detected by TD-GC-MS, as expected.

One false negative was recorded (primary trap for site 3 at 370 mL.min⁻¹ sampling flow rate), which related to a naphthalene content of only 11 ng over the entire trap, thus the amount of naphthalene in the top 5 mm spot of the trap, as analysed by LIF, was below the detection limit.

Elevated fluorescence signals at $\lambda > 323$ nm were noted for the site 2 secondary trap obtained at a 184 mL.min⁻¹ sampling flow rate, which also indicates the possibility of the

presence of other fluorophores. A correct LIF negative screening result was still obtained for this trap, as the fluorescence signal at 323 nm was not above blank levels.

Thus overall, LIF proved to be a useful screening tool in this application, and it should be noted that false positives are more acceptable than false negatives in such an environmental screening application, where a worst case scenario should be provided.

Upon further analysis of the TD-GC-MS data using the NIST library for tentative analyte identification, 1- and 2-methylnaphthalene were noted in some of the primary traps (qualifier matches of > 85) from sampling sites 1 and 3. In addition, volatile organic compounds (VOCs), specifically benzene adducts such as phenols and indene, were found in most of the traps from sites 1 and 3.

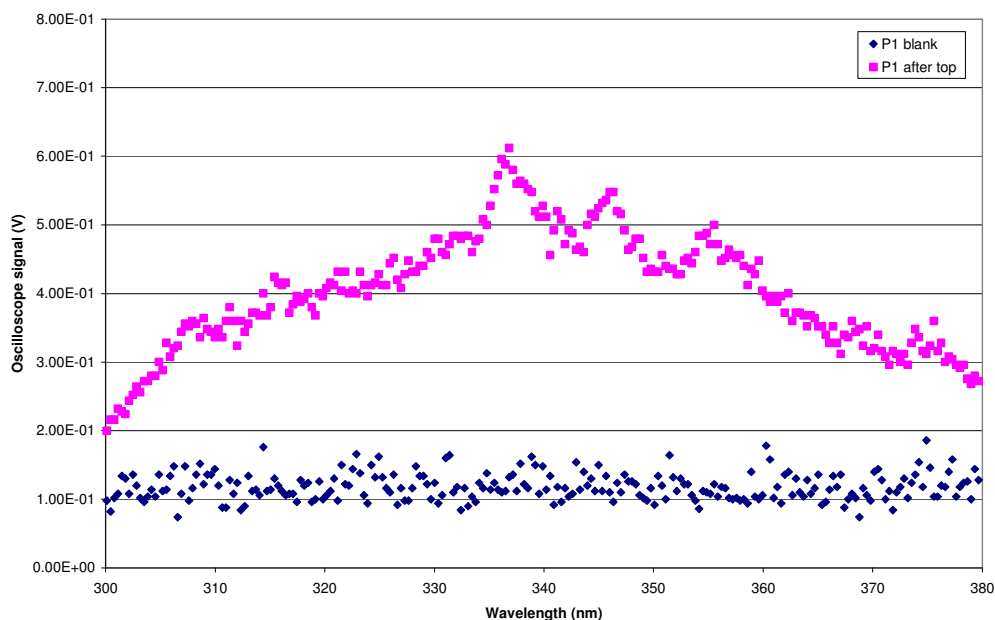


Figure 5.7: Laser induced fluorescence spectra of a primary trap before and after sampling at site 3 (31.9 ℓ of air was sampled over 25 min, LIF excitation at 292 nm).

5.6 CONCLUSION

The LIF PAH screening method and multi-channel silicone rubber trap denuder technology were tested in various applications, which demonstrated the practical use of the method at relevant environmental concentrations. The detected naphthalene concentration in

the primary traps ranged from $1.8 \mu\text{g}\cdot\text{m}^{-3}$ (diesel vehicular emissions) to $26 \mu\text{g}\cdot\text{m}^{-3}$ (industrial emissions).

The domestic cooking fire emission monitoring results revealed that naphthalene was the most abundant PAH generated and that breakthrough of this analyte was unlikely with a 2.6ℓ sampling volume. Naphthalene was not particle associated in the freshly formed smoke sample, and no less volatile PAHs were detected. Although the fuel burning was being conducted outdoors in our experiment, indoor fuel burning is also common in South Africa and may incur health effects.

The diesel vehicle exhaust monitoring experiments indicated that there was no adsorption of gas phase naphthalene onto filters during sampling, as the same amount of naphthalene was collected in the primary trap of the trap-trap configuration and in the trap of the tube-filter-trap configuration. Visual inspection of the filters and traps showed that particles had been successfully collected on the filters and had not been lost in the primary trap. No breakthrough of naphthalene was evident in the secondary traps at the sample volumes employed ($\leq 4.9 \ell$), which were larger than that used in the household fire emission experiment. Again naphthalene was not particle associated and no less volatile PAHs were detected at these low sampling volumes, although gas phase naphthalene was successfully collected.

The multi-channel silicone rubber trap denuder system and the LIF screening method were successfully tested in the sugar cane burn application, where PAH partitioning between the gas and particle phase was evident. These experiments also demonstrated that the system can be exposed to highly particle-laden atmospheres with minimal interference from the particle content.

The LIF results of the traps showed a naphthalene concentration profile through the sampling system, with possible overlap of heavier PAH emission spectra at the inlet side of the first trap. The samples therefore screened positive for naphthalene via the LIF method, indicating the need for quantitative GC-MS analysis. This experiment proved the concept of our LIF method as a screening tool and showed that enhanced resolution by spectral deconvolution by the sequential subtraction of spectra may be possible and should be further

investigated. Breakthrough occurred with respect to naphthalene at the 5 ℓ sampling volume, which was evident from both the LIF and TD-GC-MS results. The long term stability testing of stored samples containing naphthalene was also successful.

The various sampling flow rates and sample volumes used in the industrial monitoring experiments again allowed for the successful confirmation of the laboratory derived naphthalene breakthrough volume, as it was evident that breakthrough only occurred at the highest sampling volume and flow rate (31.9 ℓ sample volume).

The LIF screening method allowed for the differentiation between impacted and non-impacted industrial sampling sites, as is required of such a method. Three false positives were recorded with the LIF screening, which may have been due to the presence of non-target fluorescent compounds. One false negative was recorded where the naphthalene concentration was below the LIF detection limit. It should be noted that false positives are more acceptable than false negatives in such an environmental screening application, where a worst case scenario should be provided.

The multi-channel silicone rubber trap denuder technology and LIF screening method were therefore tested in various applications where sources were of relevance in the South African context. It is clear that breakthrough of naphthalene occurred at sampling volumes > 5 ℓ, although larger sampling volumes than this are required for sufficient pre-concentration of the lower concentration, less volatile PAHs in order to ensure that they are above the TD-GC-MS detection limit. It may therefore be necessary to sample in duplicate (one low sample volume and one higher sample volume) in order to allow for accurate quantitation by a suitable TD-GC-MS method across the range of PAH concentrations and volatilities.

Total transfer and detection of collected analyte is possible with our TD-GC-MS method, which enhances detection limits and allows for shorter sampling times and flow rates and the denuder sampling system provides particle and gas phase concentrations. It has been demonstrated that our method performs well in real practical applications and PAH concentrations.

The experiments also verified the importance of naphthalene as an indicator for atmospheric PAHs, as the TD-GC-MS results showed that naphthalene was the most abundant

PAH in the various applications which were investigated. This validates our focus on utilising the LIF method to screen for naphthalene.

5.7 REFERENCES

- Ballentine, D.C., Macko, S.A., Turekian, V.C., Gilhooly, W.P. and Martincigh, B., *Organic Geochemistry*, **1996**, 25 (1), 97-104.
- Benner, B.A., Gordon, G.E. and Wise, S.A., *Environmental Science and Technology*, **1989**, 23, 1269-1278.
- Blumer, M., Blumer, W. and Reich, T., *Environmental Science and Technology*, **1977**, 11 (12), 1082-1084.
- Boubel, R.W. and Ripperton, L.A., *Journal of the Air Pollution Control Association*, **1963**, 13 (11), 553-557.
- Boström, C.-E., Gerde, P., Hanberg, A., Jernström, B., Johansson, C., Kyrklund, T., Rannug, A., Törnqvist, M., Victorin, K. and Westerholm, R., *Environmental Health Perspectives*, **2002**, 110 (Suppl. 3), 451-488.
- De Almeida Azevedo, D., dos Santos, C.Y.M. and de Aquino Neto, F.R., *Atmospheric Environment*, **2002**, 36, 2383-2395.
- Department of Environmental Affairs and Tourism, 21 April **2006**, Government Gazette No. 28732, Notice No. 365.
- dos Santos, C.Y.M., de Almeida Azevedo, D. and de Aquino Neto, F.R., *Atmospheric Environment*, **2002**, 36, 3009-3019.
- Gachanja, A.N. and Worsfold, P.J., *The Science of the Total Environment*, **1993**, 138, 77-89.
- Gluckman, J.C., Shelly, D.C. and Novotny, M.V., *Analytical Chemistry*, **1985**, 57, 1546-1552.
- Godoi, A.F.L., Ravindra, K., Godoi, R.H.M., Andrade, S.J., Santiago-Silva, M., Van Vaeck, L. and Van Grieken, R., *Journal of Chromatography A*, **2004a**, 1027, 49-53.
- Godoi, R.H.M., Godoi, A.F.L., Worobiec, A., Andrade, S.J., de Hoog, J., Santiago-Silva, M.R. and Van Grieken, R., *Microchimica Acta*, **2004b**, 145, 53-56.
- Gustafson, P., Östman, C. and Sällsten, G., *Environmental Science and Technology*, **2008**, 42 (14), 5074-5080.
- Han, X. and Naeher, L.P., *Environment International*, **2006**, 32, 106-120.
- Harrison, R.M., Smith, D.J.T. and Luhana, L., *Environmental Science and Technology*, **1996**, 30, 825-832.
- Hoffmann, D. and Wynder, E.L., *Journal of the Air Pollution Control Association*, **1963**, 13 (7), 322-327.
- Jenkins, B.M., Jones, A.D., Turn, S.Q., and Williams, R.B., *Atmospheric Environment*, **1996**, 30 (22), 3825-3835.

- Koziel, J.A., Odziemkowski, M. and Pawliszyn, J., *Analytical Chemistry*, **2001**, 73, 47-54.
- Krieger, M.S. and Hites, R.A., *Environmental Science and Technology*, **1992**, 26, 1551-1555.
- Lemieux, P.M., Lutes, C.C. and Santoianni, D.A., *Progress in Energy and Combustion Science*, **2004**, 30, 1-32.
- Lipsky, E.M. and Robinson, A.L., *Environmental Science and Technology*, **2006**, 40, 155-162.
- Lipsky, E.M. and Robinson, A.L., *Aerosol Science and Technology*, **2005**, 39, 542-553.
- Lu, R., Wu, J., Turco, R.P., Winer, A.M., Atkinson, R., Arey, J., Paulson, S.E., Lurmann, F.W., Miguel, A.H. and Eiguren-Fernandez, A., *Atmospheric Environment*, **2005**, 39, 489-507.
- Marr, L.C., Grogan, L.A., Wöhrnschimmel, H., Molina, L., Molina, M.J., Smith, T.J. and Garshick, E., *Environmental Science and Technology*, **2004**, 38 (9), 2584-2592.
- Marr, L.C., Kirchstetter, T.W., Harley, R.A., Miguel, A.H., Hering, S.V. and Hammond, S.K., *Environmental Science and Technology*, **1999**, 33, 3091-3099.
- Mazzoli-Rocha, F., Magalhães, C.B., Malm, O., Saldiva, P.H.N., Zin, W.A. and Faffe, D.S., *Environmental Research*, **2008**, 108(1), 35-41.
- Nikolaou, K., Masclat, P. and Mouvier, G., *Science of the Total Environment*, **1984**, 32, 103-132.
- Pedersen, P.S., Ingwersen, J., Nielsen, T. and Larsen, E., *Environmental Science and Technology*, **1980**, 4 (1), 71-79.
- Rhead, M.M. and Hardy, S.A., *Fuel*, **2003**, 82, 385-393.
- Smith, K.R., Aggarwal, A.L. and Dave, R.M., *Atmospheric Environment*, **1983**, 17 (11), 2343-2362.
- South African Sugar Association, **2006**, Sugar Industry Directory for 2005/2006, accessed on 10 August 2007 at www.sasa.org.za
- Stenberg, U.R., Chapter 4: PAH emissions from automobiles in *Handbook of Polycyclic Aromatic Hydrocarbons*, Ed. Bjorseth, A., **1985**, 2, 87-111.
- USA EPA, **2002**, Health Assessment Document for Diesel Engine Exhaust. U.S. Environmental Protection Agency, Office of Research and Development, National Center for Environmental Assessment, Washington Office, Washington, DC, EPA/600/8-90/057F.
- USA EPA, **1996** (October), AP 42, 5th edition, Volume 1, Chapter 13: Miscellaneous sources, Supplement B, accessed on 8 September 2007 at www.epa.gov/ttn/chief/ap42/ch13
- Viau, C., Hakizimana, G. and Bouchard, M., *International Archives of Occupational and Environmental Health*, **2000**, 73, 331-338.
- Wild, S.R. and Jones, K.C., *Environmental Pollution*, **1995**, 88, 91-108.
- Wu, W.Z., Wang, J.X., Zhao, G.F. and You, L., *Journal of Environmental Science and Health*, **2002**, A37 (4), 579-600.



Zamperlini, G.C.M., Silva, M.R.S. and Vilegas, W., *Chromatographia*, **1997**, 46 (11/12), 655-663.

Zielinska, B., Sagebiel, J., Arnott, W.P., Rogers, C.F., Kelly, K.E., Wagner, D.A., Lighty, J.S., Sarofim, A.F. and Palmer, G., *Environmental Science and Technology*, **2004**, 38, 86-90.